Hindawi
Mathematical Problems in Engineering
Volume 2021, Article ID 5579541, 14 pages
https://doi.org/10.1155/2021/5579541

Research Article

L_1 Adaptive Fractional Control Optimized by Genetic Algorithms with Application to Polyarticulated Robotic Systems

Boutheina Maalej,[1,2,3] **Rim Jallouli Khlif**,[1,4] **Chokri Mhiri**,[2,5,6] **Mohamed Habib Elleuch**,[2,7] **and Nabil Derbel**[1,3]

[1]*University of Sfax, ENIS, Laboratory of Control & Energy Management, Sfax, Tunisia*
[2]*Clinical Investigation Center, Sfax, Tunisia*
[3]*Digital Research Center of Sfax, Sfax, Tunisia*
[4]*Higher Institute of Computer Science and Multimedia of Sfax, ISIMS, Sfax, Tunisia*
[5]*Department of Neurology, Hospital Habib Bourguiba, Sfax, Tunisia*
[6]*Neuroscience Laboratory, Faculty of Medicine, Sfax University, Sfax, Tunisia*
[7]*Research Unit: Les Pathologies de L'Appareil Locomoteur, Service de Medecine Physique et de Readaptation, CHU Habib Bourguiba, Sfax, Tunisia*

Correspondence should be addressed to Boutheina Maalej; boutheina.maalej@stud.enis.tn

Received 1 March 2021; Revised 20 March 2021; Accepted 25 March 2021; Published 10 April 2021

Academic Editor: Omar Naifar

Recently, an adaptive control approach has been proposed. This approach, named L_1 adaptive control, involves the insertion of a low-pass filter at the input of the Model Reference Adaptive Control (MRAC). This controller has been designed to overcome several limitations of classical adaptive controllers such as (i) the initialization of estimated parameters, (ii) the stability problems with high adaptation gains, and (iii) the appropriate parameter excitation. In this paper, a new design of the filter is presented, used for L_1 adaptive control, for which the desired performances are guaranteed (appropriate values of the control during start-up, a high filtering of noises, a reduced time lag, and a reduced energy consumption). Parameters of the new proposed filter have been optimised by genetic algorithms. The proposed L_1 adaptive fractional control is applied to a polyarticulated robotic system. Simulation results show the efficiency of the proposed control approach with respect to the classical L_1 adaptive control in the nominal case and in the presence of a multiplicative noise.

1. Introduction

Conventional adaptive controllers such as the Model Reference Adaptive Controller [1] (MRAC) are lacking robustness. In fact, among the drawbacks of these controllers is the choice of the adaptation gains. A higher adaptation gain yields to a high gain controller with good performances and tracking properties but poor robustness to unmodeled actuator dynamics [2]. In [3, 4] and [5], researchers have discussed the robustness of different architectures and schemes of adaptive controllers [6]. To overcome these limitations [7, 8] that adaptive controllers are facing, the L_1 adaptive controller was proposed in [9, 10]. The basic part of the L_1 adaptive control is the presence of the low-pass filter introduced in the control channel. It is the trade-off between performance and robustness. As a result, the L_1 adaptive control architecture [11] differs from the standard adaptive control by its particular architecture, where adaptation and robustness are decoupled [12]. Hence, even with an increasing adaptation gain, the closed-loop system can be enhanced without the degradation of the robustness. Among the drawbacks of the L_1 adaptive control is the time lag. Researchers in [13–15] have proposed to add different supplementary controllers aiming to eliminate the appearing time lag. In this paper, the proposed contribution is the L_1 adaptive fractional control based on fractional calculus [16–19]. Then, the new idea is to carefully

choose the filter. In fact, instead of using integer-order filters [20], this paper proposes the use of fractional-order filters [21]. Fractional-order filters [22, 23] have many advantages; they tune the shaper bandwidth and ensure a better selectivity. Moreover, the use of fractional orders in a lot of applications [24, 25], where the system is extremely complex, allows solving huge problems such as reducing high control values. In this paper, L_1 fractional adaptive control is implemented, and it has proved a reduction of the error (elimination of the time lag) and reduction of the energy consumption.

The new approach, based on fractional filters [26], is then implemented on a dynamical model of an exoskeleton and simulation results are presented. Good performances validate the L_1 adaptive fractional controller. Moreover, the parameters of these filters have been optimized by genetic algorithms [27, 28].

The rest of this paper is organized as follows. In Section 2, a background on fractional-order systems is presented. Section 3 presents a background on L_1 adaptive control. Section 4 is dedicated to the validation of the main contribution by the application to a polyarticulated robotic system. First, the problem formulation is detailed. Then, performance evaluation criteria are established for the case of an exoskeleton in the nominal case and then in the presence of a multiplicative noise in order to test the robustness of the proposed controller. Section 5 gives the final conclusion.

2. Background on Fractional-Order Systems

Oustaloup's recursive approximation algorithm is presented in this section. This method deals with the frequency space and it is based on a recursive distribution of negative real zeros and poles in order to guarantee a minimal phase behavior [29]. The aim is to synthesize the rational function in the frequency range $[\omega_L, \omega_H]$:

$$D(s) = \left(\frac{s}{\omega_L}\right)^r, \quad r \in]-1; 0[, \tag{1}$$

using a recursive distribution of zeros and poles as:

$$\widetilde{D}(s) = \prod_{k=-N}^{N} \left(\frac{1 + s/\omega_k'}{1 + s/\omega_k}\right), \tag{2}$$

where $\{-\omega_k', -\omega_k\}$ is the pair of the zero and the pole of order k expressed as

$$\omega_k' = \omega_L \sqrt[2N+1]{\left(\frac{\omega_H}{\omega_L}\right)^{\alpha_k - 0.5r}}, \tag{3}$$

$$\omega_k = \omega_L \sqrt[2N+1]{\left(\frac{\omega_H}{\omega_L}\right)^{\alpha_k + 0.5r}}, \tag{4}$$

where $\alpha_k = k + N + 0.5$, with the following:

ω_L is the high transitional frequency

ω_H is the low transitional frequency

and $2N + 1$ is the total number of recursive poles and zeros. The gain of the filter is equal to the unity for $\omega < \omega_L$.

For a good approximation of the fractional-order filter, two or three decades at least should be considered between ω_L and ω_H.

3. Background on L_1 Adaptive Control

The L_1 adaptive control [30] is designed as shown in the block diagram of Figure 1. A square system is considered with an input vector $u \in \mathbb{R}^m$ and an output vector $y \in \mathbb{R}^m$. The desired output and the desired output velocity vectors are, respectively, y_d and $\dot{y}_d$. The dynamic system is described as

$$\ddot{y} = a_1 y + a_2 \dot{y} + bu + b'\theta, \tag{5}$$

with θ is a nonlinear function that gathers all the nonlinearities of the system and b is a regular matrix. a_1 and a_2 are square matrices with the appropriate dimension.

The generalized tracking error is defined as follows:

$$\rho = (\dot{y} - \dot{y}_d) + \Lambda(y - y_d), \tag{6}$$

with $\Lambda \in \mathbb{R}^{m \times m}$ being a positive definite diagonal matrix. The control input vector $u(t)$ is

$$u(t) = b^{-1}[u_m(t) + u_{ad}], \tag{7}$$

with

$$u_m(t) = b^{-1}[A_m \rho(t) - a_1 y - a_2 \dot{y} + \ddot{y}_d) - \Lambda(\dot{y} - \dot{y}_d)], \tag{8}$$

where

$A_m \in \mathbb{R}^{m \times m}$ is a Hurwitz matrix that characterizes the desired transient response of the system

$u_{ad} \in \mathbb{R}^m$ is an adequate adaptive term

The time derivative of (6) leads to the following equation:

$$\dot{\rho} = bu(t) + b'\theta - \ddot{y}_d + \Lambda(\dot{y} - \dot{y}_d). \tag{9}$$

Then,

$$\dot{\rho} = A_m \rho(t) + u_{ad}(t) + b'\theta(t). \tag{10}$$

The adaptive control is defined in order to cancel the nonlinearity $\theta(t)$. For that, in order to estimate and compensate the term $\theta(t)$, let us consider the following state predictor:

$$\dot{\widehat{\rho}} = A_m \widehat{\rho}(t) + u_{ad}(t) + b'\widehat{\theta}(t) - K\widetilde{\rho}(t), \tag{11}$$

where

$\widehat{\theta}(t)$ is the estimation of the nonlinear term θ

$\widetilde{\theta}(t) = \widehat{\theta}(t) - \theta(t)$ is the error of the nonlinear term θ

$\widetilde{\rho}(t) = \widehat{\rho}(t) - \rho(t)$ is the prediction error

$K \in \mathbb{R}^{m \times m}$ is a designed matrix introduced to reject high-frequency noises

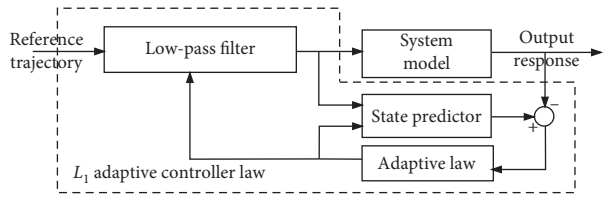

Figure 1: Block diagram of L_1 adaptive control.

$$\dot{\tilde{\rho}} = A\tilde{\rho}(t) + b'\tilde{\theta}(t), \tag{12}$$

with $A = A_m - K$ being a Hurwitz matrix defining a dynamical behavior of $\tilde{\rho}$ at least two to three times faster than A_m.

The Lyapunov function associated with the system is

$$V = \tilde{\rho}^T P\tilde{\rho} + \tilde{\theta}^T \Gamma^{-1}\tilde{\theta}, \tag{13}$$

where Γ is the positive diagonal high gain matrix and P is a definite positive matrix verifying

$$\mathrm{PA} + A^T P = -Q < 0. \tag{14}$$

Its differential with respect to time gives

$$\begin{aligned} \dot{V} &= \tilde{\rho}^T \underbrace{\left(PA + A^T P\right)}_{=-Q} \tilde{\rho} + 2\tilde{\theta}^T b'^T P\tilde{\rho} + 2\tilde{\theta}^T \Gamma^{-1}\dot{\tilde{\theta}} \\ &= -\tilde{\rho}^T Q\tilde{\rho} + 2\tilde{\theta}^T \underbrace{\left(b'^T P\tilde{\rho} + \Gamma^{-1}\dot{\tilde{\theta}}\right)}_{=0} = -\tilde{\rho}^T Q\tilde{\rho} \le 0. \end{aligned} \tag{15}$$

Hence,

$$\dot{\tilde{\theta}} = -\Gamma b'^T P\tilde{\rho}. \tag{16}$$

The estimate of $\theta(t)$, $\hat{\theta}(t)$ is obtained using the projection operator which prevents the estimated values from exceeding their admissible range specified in the control design:

$$\dot{\hat{\theta}}(t) = \mathrm{Proj}\left[\hat{\theta}(t), -\Gamma b'^T P\rho(t)\right]. \tag{17}$$

The adaptive control term is as follows:

$$u_{ad}(s) = -C(s)b'\hat{\theta}(s), \tag{18}$$

where $\hat{\theta}(s)$ is the Laplace transform of $\hat{\theta}(t)$ and $C(s)$ is a BIBO (bounded-input bounded-output) stable transfer function.

4. Proposed L_1 Adaptive Fractional Control Applied to Polyarticulated Robotic Systems

4.1. Main Contribution. In general, the standard integer-order filters used for the L_1 adaptive control generate

(i) High values of the control during start-up

(ii) High energy consumption

(iii) A small filtering of noises

(iv) An important time lag

For these reasons, the main proposition is to replace these filters by fractional-order ones that are realised by a sequence of first-order systems. The real order of the fractional system is equal to $2N + 1$.

This makes the system slower during its start-up and consequently generates appropriate values of the control during start-up, a high filtering of noises, and a reduced time lag.

The transfer functions of all considered filters in this paper will be implemented and compared. They are defined as

$$C_{-1}(s) = \frac{1}{1 + \tau s}, \tag{19}$$

$$C_{-2}(s) = \frac{1}{(1 + \tau s)^2}, \tag{20}$$

$$C_r(s) = \left(\frac{1 + s/\omega_L}{1 + s/\omega_H}\right)^r, \quad r \in]-2, -1[\cup]-1, 0[, \tag{21}$$

where C_{-1} and C_{-2} filters can be represented as C_r, for high values of ω_H, and $\tau\omega_L = 1$.

4.2. Problem Formulation of the Exoskeleton. In this paper, we are interested in the control of polyarticulated robotic systems for which the dynamic model can be written in the following form:

$$M(q)\ddot{q} + F(q, \dot{q}) = \tau, \tag{22}$$

where

$M(q) \in \mathbb{R}^{n\times n}$ is the inertia matrix

$F(q, \dot{q}) \in \mathbb{R}^n$ is the vector of the Coriolis, centrifugal, gravitational, and contact forces

$\tau \in \mathbb{R}^n$ is the vector of torques generated by actuators

$q = [q_1\, q_2, \ldots, q_n]^T \in \mathbb{R}^n$ is the position vector

$\dot{q} = [\dot{q}_1\, \dot{q}_2, \ldots, \dot{q}_n]^T \in \mathbb{R}^n$ is the velocity vector

$\ddot{q} = [\ddot{q}_1\, \ddot{q}_2, \ldots, \ddot{q}_n]^T \in \mathbb{R}^n$ is the acceleration vector

The proposed control algorithm, namely, the L_1 adaptive fractional control, is implemented on two-degrees-of-freedom lower limb exoskeleton [31], which is dedicated to the rehabilitation of cerebral palsy kids aged from two to ten years. Hence, the dynamic parameters are chosen as the mean values of lengths and masses (Table 1).

4.3. Parameters Optimization by Genetic Algorithms. The choice of the filters' coefficients is the most important and essential part. In fact, they should be chosen to ensure the minimality of errors. For this purpose, an algorithm of optimization is proposed to determine these coefficients. Several numerical methods have been formulated from the minimization of a certain performance criterion to find an optimal solution such as genetic algorithms [32–34]. For a minimization problem of a criterion J (chosen in our case,

Table 1: Summary of the dynamic parameters of the lower limb exoskeleton.

Parameters	Values
Mass of the exoskeleton	1 kg
Mean value of thigh length of the human limb	0.282 m
Mean value of shank length of the human limb	0.282 m
Mean value of thigh mass of the human limb	1.082 kg
Mean value of shank mass of the human limb	3.535 kg
Exoskeleton inertia	1.24×10^{-3} kg m^2
Thigh inertia of human limb	8.78×10^{-3} kg m^2
Shank inertia of human limb	2.73×10^{-3} kg m^2

the tracking error), a genetic algorithm can proceed as follows [35]:

(1) Choice of a random generation of N_i individuals

(2) Evaluation of the individuals by computing their fitness translating the performance index to be optimized

(3) Cross of two parents with a probability to generate two children

(4) Mutation of the two parents with a probability

(5) Selection of best N_i solutions

(6) Evaluation of the new individuals

(7) Repetition of steps (3), (4), (5), and (6) until the new individuals are too close giving the same fitness or reaching the maximum number of iterations.

The aim of this work is the determination of the filters' parameters. The best parameters are those that give the lowest tracking error. A population of $N_i = 20$ individuals and 30 generations is chosen. The initial populations of the different parameters are as follows:

r: between 0.1 and 0.95

ω_L: between 1 and 100

ω_H: between $10^2 \times \omega_L$ and $10^5 \times \omega_L$

The algorithm has been converged to the following results:

$r = -1$ for C_{-1} (first-order filter)

$r = -2$ for C_{-2} (second-order filter)

$r = -0.88$ for $C_{-0.88}$ (fractional-order filter)

$r = -1.87$ for $C_{-1.87}$ (fractional-order filter)

Fixed $\omega_L = 19$ rad/s and $\omega_H = 80000$ rad/s for all cases

4.4. Performance Evaluation Criteria. One of our main objectives is to improve the precision and to increase the tracking accuracy of the lower limb exoskeleton through the proposed controller. Hence, let us define some performance indices in order to quantify the relevance of the proposed new L_1 adaptive fractional controller. The integral of the absolute error (IAE) and the relative integral of the absolute error (IAER) are accuracy evaluation tools used to evaluate the difference between the desired trajectory and the actual one during a specified time interval $[t_1, t_2]$ ($e = q_d - q$ denotes the tracking error). Moreover, it is very important to evaluate the energy consumption for the proposed controller. The evaluation criteria are defined as

$$\mathrm{IAE} = \int_{t_1}^{t_2} |e| \mathrm{d}t, \tag{23}$$

$$\mathrm{IAER} = \frac{\int_{t_1}^{t_2} |e| \mathrm{d}t}{\int_{t_1}^{t_2} |q_d| \mathrm{d}t}, \tag{24}$$

$$\mathrm{IAU} = \int_{t_1}^{t_2} |\tau| \mathrm{d}t, \tag{25}$$

$$\mathrm{ISU} = \int_{t_1}^{t_2} \tau^2 \mathrm{d}t. \tag{26}$$

4.4.1. Numerical Simulation Results

(1) Scenario 1: Nominal Case. In this section, simulation results will be presented in the nominal case. Two specific intervals are considered, defined by the following:

The interval $[t_1, t_2] = [0, 0.5]\,s$ describes the start-up duration, corresponding to the transient response

The interval $[t_1, t_2] = [1, 2]\,s$ describes a steady-state period (a steady-state period describes the behavior of the system during one period of the steady-state response)

The gait cycles of the hip and knee joints versus time are plotted in Figures 2 and 3 for the L_1 adaptive controller with different filters. Then, Figures 4 and 5 show the hip and knee joints tracking errors. It is clear from these figures that the time lag that appeared while using the classical L_1 adaptive control has been eliminated thanks to the fractional-order filter. In fact, for the hip and the knee joints, the error is too high while using the standard filters (first- or second-order filter); however, the error becomes small and does not exceed 1° while using integral fractional-order filters (in case of $C_{-0.88}$ filter).

In the following, performance values regarding the hip joint are indexed by 1 and those of the knee joint by 2. Figure 6 shows the integral of the absolute errors IAE and IAER versus the filter order r.

The use of the integral fractional filter $C_{-0.88}$ shows an improvement of 85.23% and 43.38% for the hip and knee joints, respectively, in terms of the tracking precision with regard to the first-order filter (see Table 2) and 90.31% and 69.82% with regard to the second-order filter. Moreover, the fractional filter $C_{-1.87}$ proves an improvement in terms of the tracking error about 29% and 46.04% for the hip and knee joints, respectively, with regard to the second-order filter.

Figures 7 and 8 depict the generated control input torques of the hip and knee joints. Figure 9 presents the maximum values of the torques while using L_1 adaptive controller with different filters. In terms of energy consumption, Figures 9 and 10 show clearly that there is a considerable difference between filters during the start-up

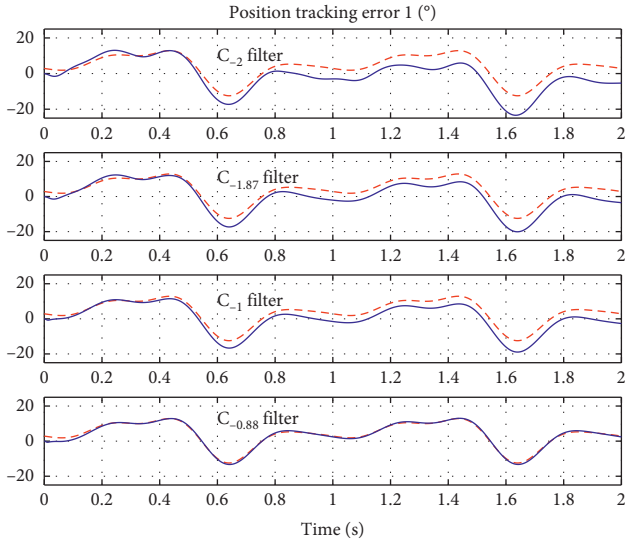

Figure 2: Evolution of the hip joint tracking versus time. Dashed line: desired trajectory; continuous line: actual trajectory.

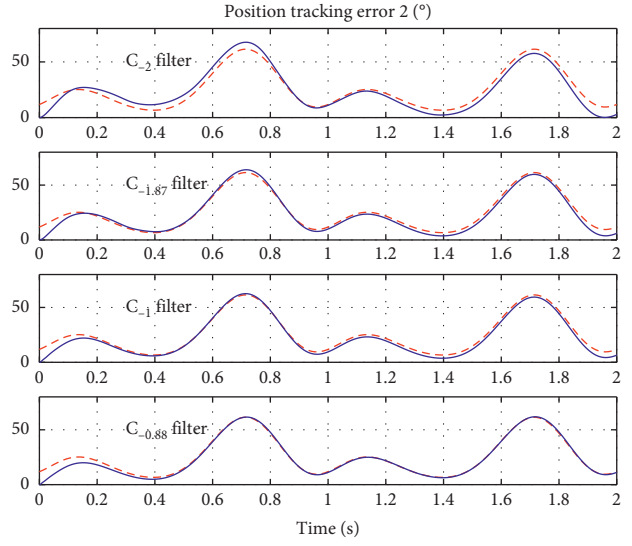

Figure 3: Evolution of the knee joint tracking versus time. Dashed line: desired trajectory; continuous line: actual trajectory.

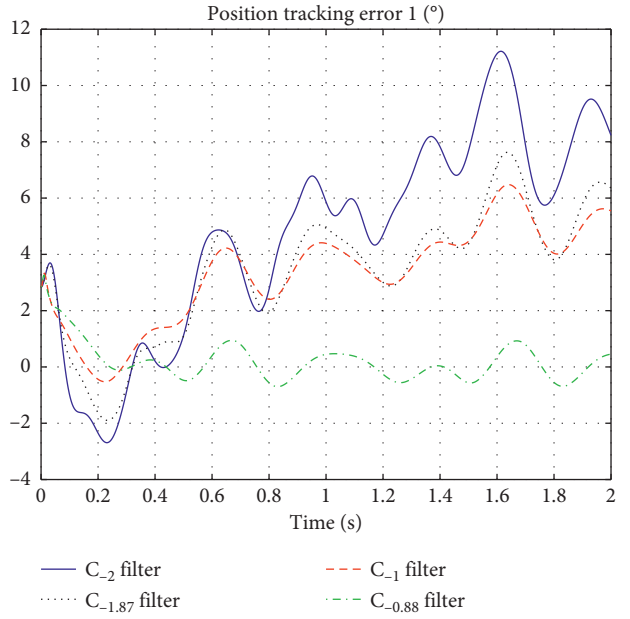

Figure 4: Evolution of the hip joint tracking errors versus time.

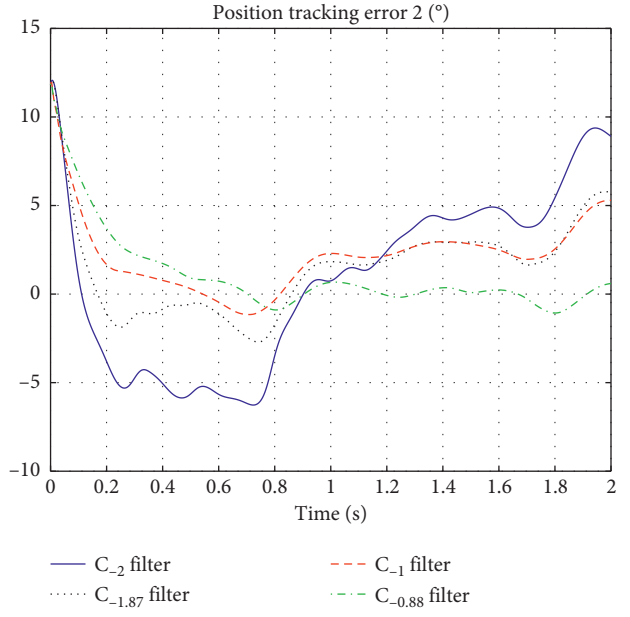

Figure 5: Evolution of the knee joint tracking errors versus time.

and the steady-state periods, respectively. The improvement percentage of the energy consumption during both phases (start-up and steady-state periods) is illustrated in Tables 3 and 4. Indeed, there is an improvement of the integral of the absolute torques IAU, 12.77% and 13.64%, while using the $C_{-0.88}$ filter with regard to the first-order filter and 38.24% and 31.06% of improvement with regard to the second-order filter, respectively, to the hip and knee joints. The integral of squared torques ISU is also improved (8.52% and 1.07% of improvement while using the $C_{-0.88}$ filter with regard to the first-order filter and about 1.28% for the hip joint with regard to the second-order filter) during start-up. Moreover, there is an improvement of IAU, about 5.08% and 4.47%, with regard to the first-order filter and 24.56% and 16.61% of improvement with regard to the second-order filter. During the steady-state period, in terms of ISU, there are 7.24% and 7.59% of improvements with regard to the first-order filter and about 40.63% and 30.28% of improvements with regard to the second-order filter.

Besides, in the case of $C_{-1.87}$, the fractional filter shows an improvement during the start-up period with regard to the first-order filter (34.04% and 40.55% of improvement for the hip and knee joints in terms of ISU) and with regard to the second-order filter with 18.52% and 14.31% of improvement for the hip and knee joints in terms of IAU and about 28.82% and 21.36% in terms of ISU. Moreover, it shows an

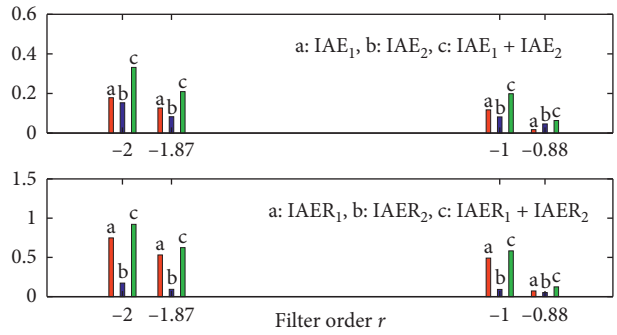

Figure 6: Clustered column chart of IAE_1, IAE_2, and $(IAE_1 + IAE_2)$, as well as $IAER_1$, $IAER_2$, and $(IAER_1 + IAER_2)$ versus the filter order r.

Table 2: Improvement quantification in % of tracking error while using fractional filters.

Filters	C_{-1}		C_{-2}	
	IAE_1	IAE_2	IAE_1	IAE_2
$C_{-0.88}$	85.23%	43.38%	90.31%	69.82%
$C_{-1.87}$	0%	0%	29%	46.04%

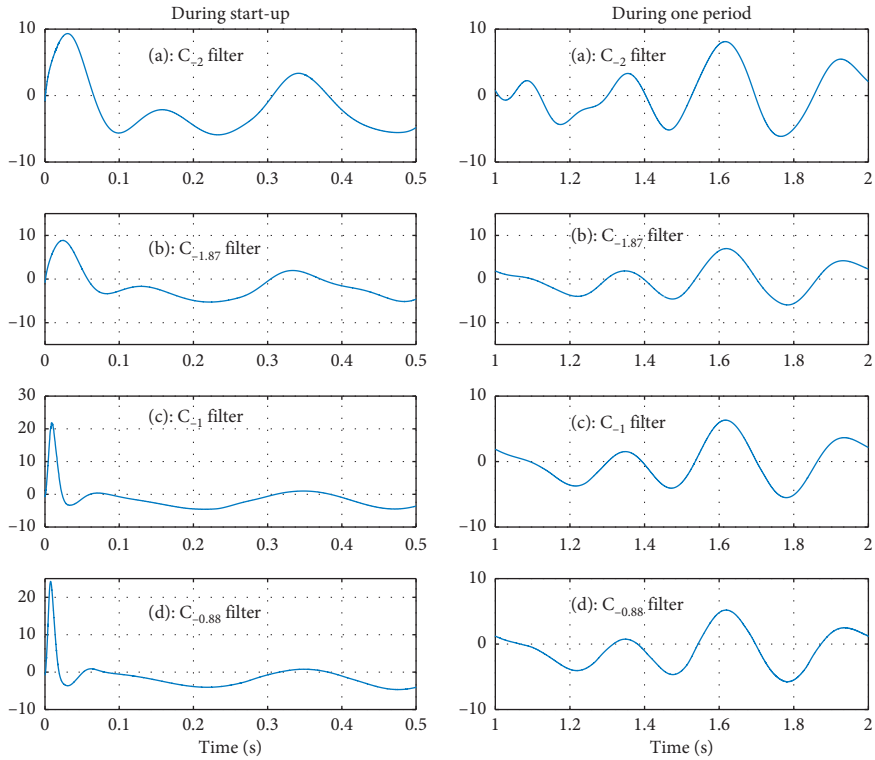

Figure 7: Evolution of the control input torques versus time of the hip joint.

improvement during the steady-state period, but it is less than $C_{-0.88}$ filter. In fact, with regard to the first-order filter, there is no improvement, and with regard to the second-order filter, about 12.9% and 7.12% improvement in terms of IAU and about 23.17% and 16.66% improvement in terms of ISU are proved.

As a result, the integral fractional filter with $-1 < r < 0$ is proved to be the filter thanks to the rate of improvement that has been shown.

(2) Scenario 2: robustness towards noise. The aim of this section is to test the robustness of the integral filter with $-1 < r < 0$ towards the standard filters (first- and second-order); hence, a multiplicative measurement noise (5%) has been added to the system. Figures 11 and 12 show the tracking gait cycles of the hip and the knee joints, respectively. It is obvious in Figures 13 and 14 that the effect of the noise is more important for the first- and second-order filters than for the fractional-order filter with $-1 < r < 0$

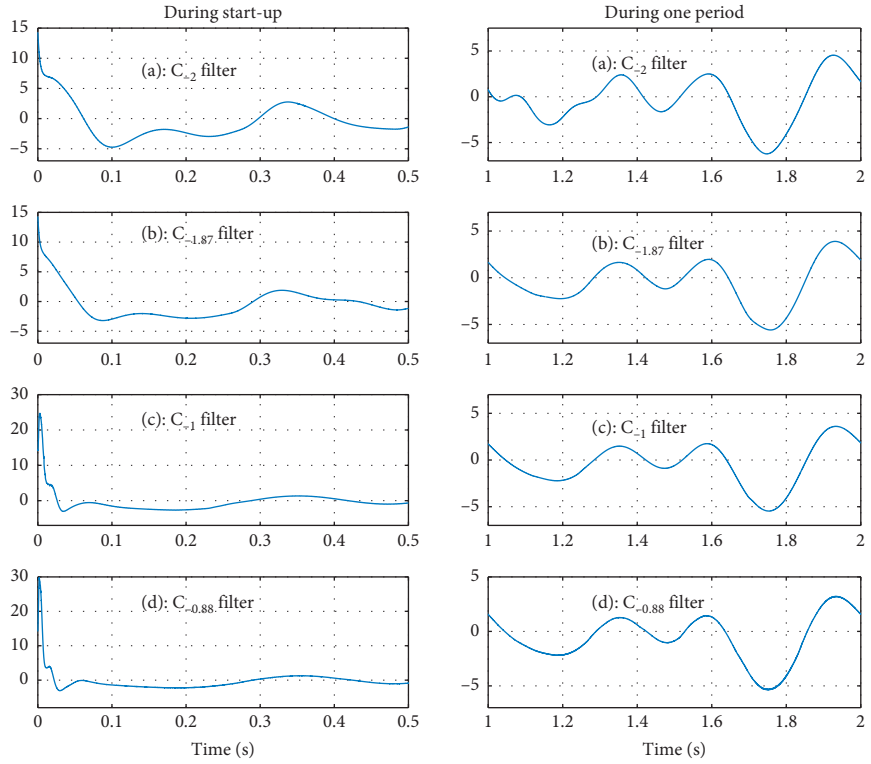

FIGURE 8: Evolution of the control input torques versus time of the knee joint.

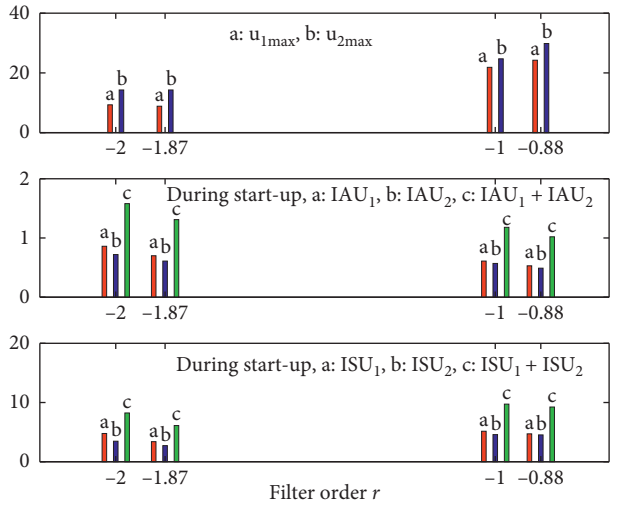

FIGURE 9: Clustered column chart of the maximum of torques ($U_{1\max}$ and $U_{2\max}$), IAU_1, IAU_2, and $(IAU_1 + IAU_2)$, as well as ISU_1, ISU_2, and $(ISU_1 + ISU_2)$ during start-up versus the filter order r.

based on the integral of the absolute errors IAE and the integral of the absolute torques IAU.

Moreover, it is obvious from Figure 15 that the integral of the absolute errors IAE is high for both standard filters. In fact, the use of the integral fractional filter $C_{-0.88}$ shows an improvement of 21% for the knee joint (during start-up) and an improvement of 90.87% and 79.39% for the hip and the knee joints, respectively (during one period), in terms of tracking precision compared to the first-order filter. With regard to the second-order filter, it shows an improvement of 15.49% for the hip joint (during start-up) and an improvement of 93.10% and 85.38% for the hip and knee joints respectively (during one period) (see Tables 5 and 6).

Figure 16 shows the maximum values of the torques for the different used filters. It is clear that the torques' values, during start-up, are comparable to previous results shown in the first scenario (Figures 17 and 18).

Tables 7 and 8 present the improvement quantification of the energy consumption while using an integral fractional order filter. In fact, in terms of the integral of the absolute

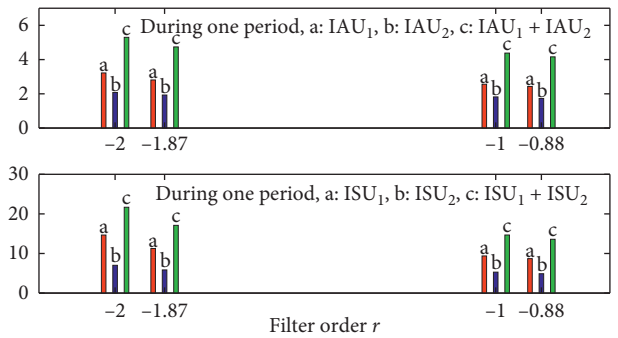

Figure 10: Clustered column chart of IAU_1, IAU_2, and $(IAU_1 + IAU_2)$, as well as ISU_1, ISU_2, and $(ISU_1 + ISU_2)$ during steady-state period versus the filter order r.

Table 3: Improvement quantification in % of energy during start-up period while using fractional filters.

Filters	C_{-1}				C_{-2}			
	IAU_1	IAU_2	ISU_1	ISU_2	IAU_1	IAU_2	ISU_1	ISU_2
$C_{-0.88}$	12.77%	13.64%	8.52%	1.07%	38.24%	31.06%	1.28%	0%
$C_{-1.87}$	0%	0%	34.04%	40.55%	18.52%	14.31%	28.82%	21.36%

Table 4: Improvement quantification in % of energy during steady-state period while using fractional filters.

Filters	C_{-1}				C_{-2}			
	IAU_1	IAU_2	ISU_1	ISU_2	IAU_1	IAU_2	ISU_1	ISU_2
$C_{-0.88}$	5.08%	4.47%	7.24%	7.59%	24.56%	16.61%	40.63%	30.28%
$C_{-1.87}$	0%	0%	0%	0%	12.9%	7.12%	23.17%	16.66%

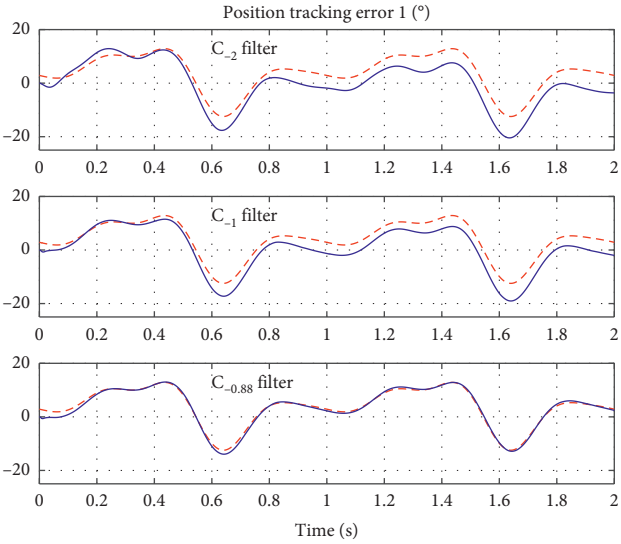

Figure 11: Evolution of the hip joint tracking versus time in the presence of 5% of noise. Dashed line: desired trajectory; continuous line: actual trajectory.

torques IAU, there is an improvement of 38.04% and 30.8% while using $C_{-0.88}$ filter with regard to the second-order filter for the hip and the knee joints, respectively, during the start-up and an improvement of 17.4% and 9.4% during the steady-state period. Moreover, there is an improvement of 11.42% and 11.96% while using $C_{-0.88}$ filter with regard to

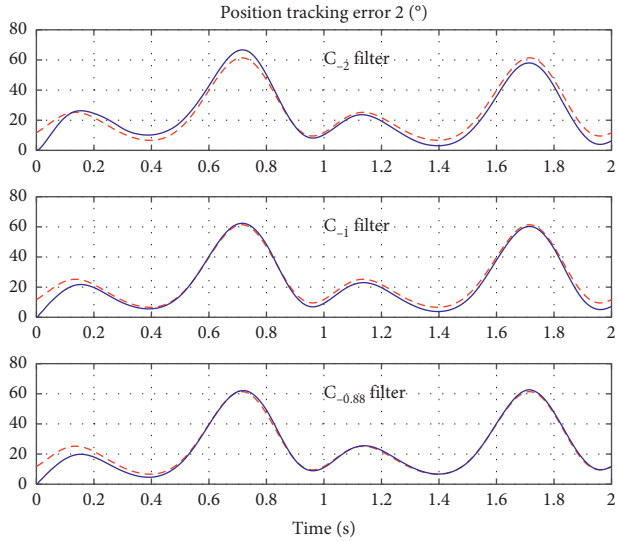

Figure 12: Evolution of the knee joint tracking versus time in the presence of 5% of noise. Dashed line: desired trajectory; continuous line: actual trajectory.

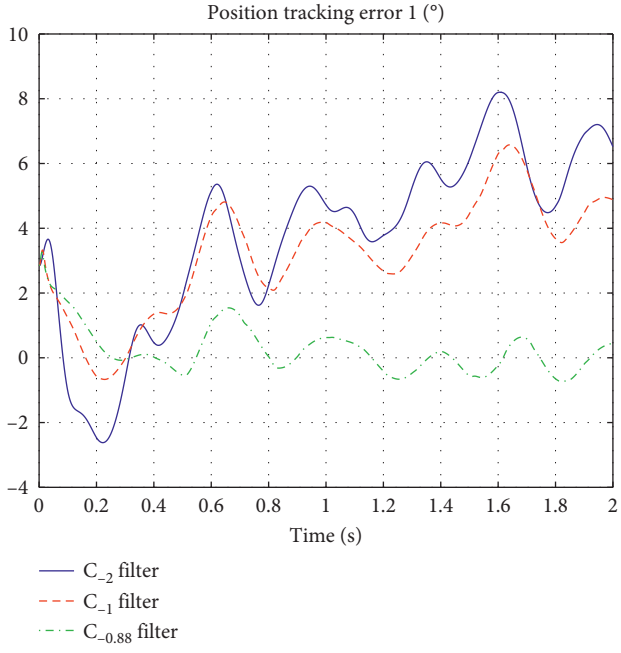

Figure 13: Evolution of the hip joint tracking error versus time in the presence of 5% of noise.

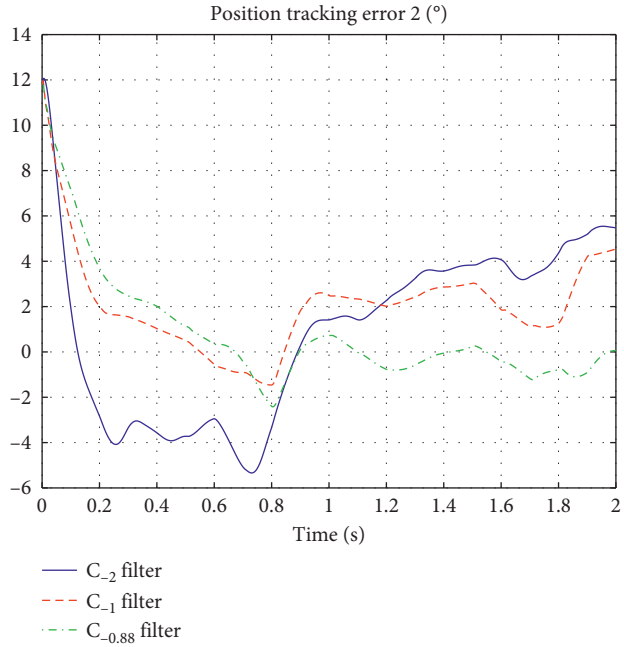

Figure 14: Evolution of the knee joint tracking error versus time in the presence of 5% of noise.

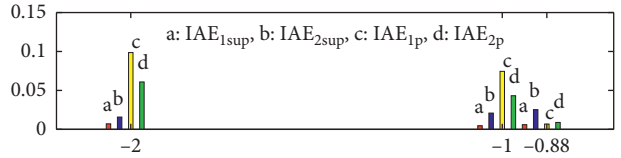

Figure 15: Clustered column chart of IAE_{1sup} and IAE_{2sup} during start-up and IAE_{1p} and IAE_{2p} during steady-state period, for both joints, versus the filter order r.

Table 5: Improvement quantification in % of tracking error while using the fractional filter in the presence of 5% noise during start-up for the hip and knee joints.

Filters	C_{-1}		C_{-2}	
	IAE_{1sup}	IAE_{2sup}	IAE_{1sup}	IAE_{2sup}
$C_{-0.88}$	0%	21%	15.49%	0%

Table 6: Improvement quantification in % of tracking error while using the fractional filter in the presence of 5% noise during one period for the hip and knee joints.

Filters	C_{-1}		C_{-2}	
	IAE_{1p}	IAE_{2p}	IAE_{1p}	IAE_{2p}
$C_{-0.88}$	90.87%	79.39%	93.10%	85.38%

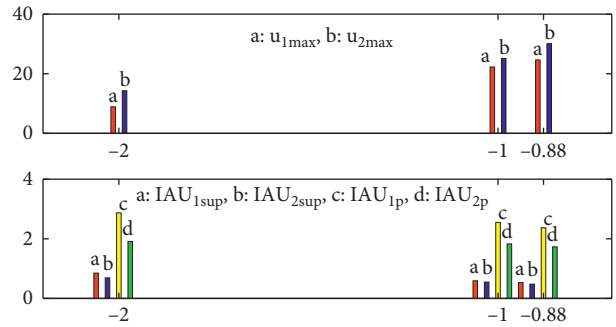

FIGURE 16: Clustered column chart of the maximum of torques ($U_{1\,\max}$ and $U_{2\,\max}$), $\mathrm{IAU}_{1\mathrm{sup}}$ and $\mathrm{IAU}_{2\mathrm{sup}}$ during start-up and IAU_{1p} and IAU_{2p} during steady-state period, for both joints, versus the filter order r.

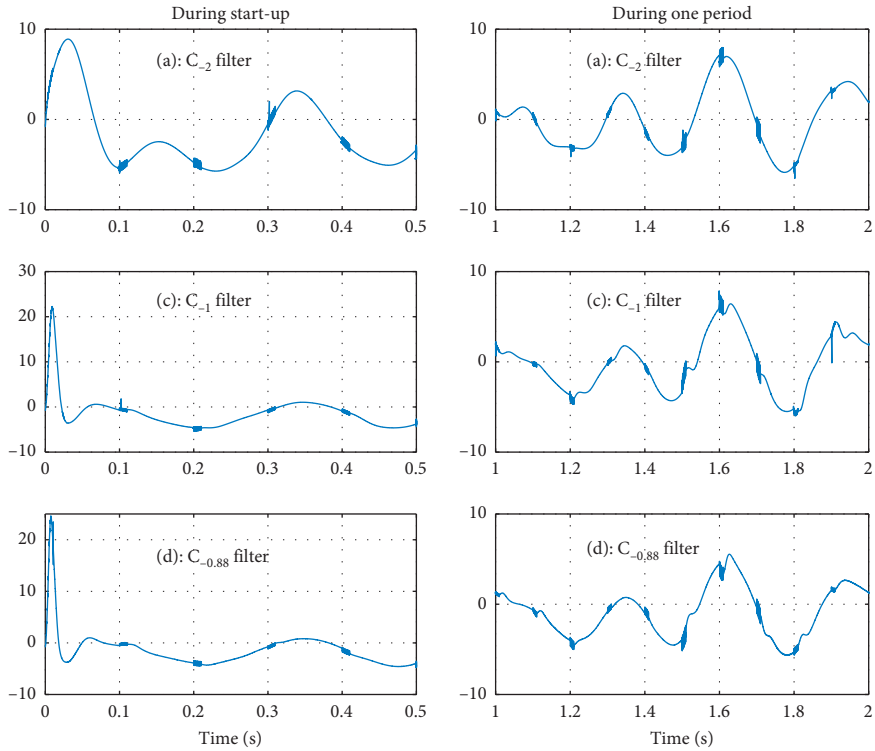

FIGURE 17: Evolution of the control input torques versus time of the hip joint in the presence of 5% of noise.

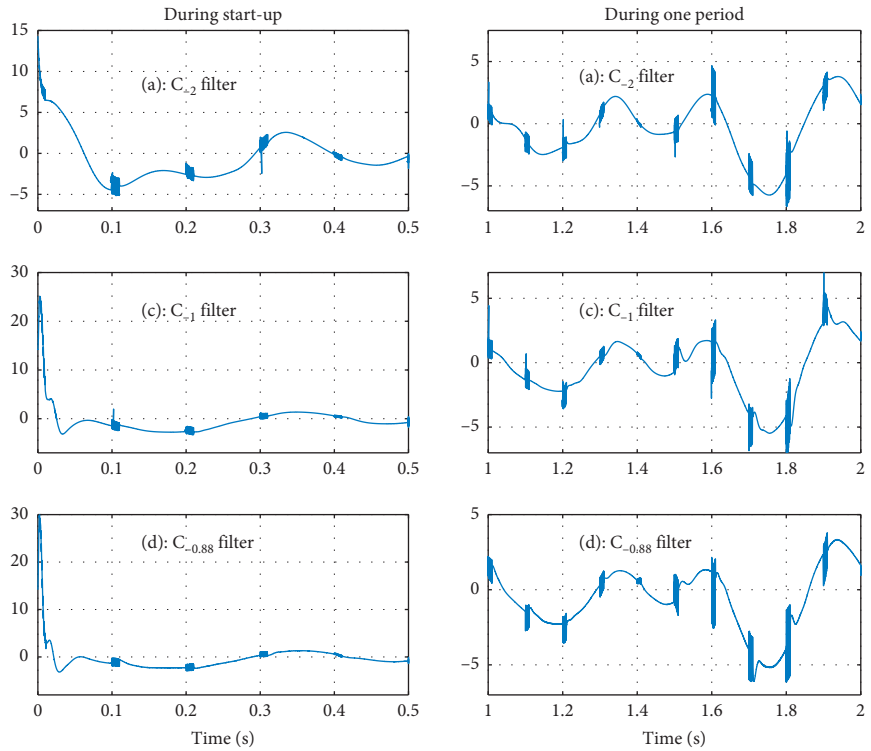

Figure 18: Evolution of the control input torques versus time of the knee joint in the presence of 5% of noise.

Table 7: Improvement quantification in % of energy while using the fractional filter in the presence of 5% noise for the hip joint during start-up and one period.

Filters	C_{-1}		C_{-2}	
	IAU_{1sup}	IAU_{1p}	IAU_{1sup}	IAU_{1p}
$C_{-0.88}$	11.42%	7.12%	38.04%	17.4%

Table 8: Improvement quantification in % of energy while using the fractional filter in the presence of 5% noise for the knee joint during start-up and one period.

Filters	C_{-1}		C_{-2}	
	IAU_{2sup}	IAU_{2p}	IAU_{2sup}	IAU_{2p}
$C_{-0.88}$	11.96%	5.58%	30.8%	9.4%

the first-order filter for the hip and the knee joints, respectively, during the start-up; and there is an improvement of 7.12% and 5.58% during the steady-state period.

5. Conclusion

In this paper, a new solution to eliminate the time lag that appears while using the L_1 adaptive control has been proposed. The new approach consists of replacing the standard integer filters, used in the L_1 adaptive control, by fractional-order filters. The proposed approach has been tested on a polyarticulated system. Simulation results show clearly better performances of the new proposed L_1 adaptive fractional control. In fact, the use of the integral fractional-order filter enhances the performances in terms of tracking error (elimination of the time lag) and energy consumption for both cases (nominal case and in the presence of a multiplicative noise). Moreover, the filter parameters have been optimized by genetic algorithms. In future works, L_1 adaptive fractional controller will be implemented on a real exoskeleton.

Data Availability

The data used to support the findings of this study are available from the corresponding author upon request.

Conflicts of Interest

The authors declare that they have no conflicts of interest.

Acknowledgments

The authors would like to acknowledge (i) the Ministry of Higher Education, Tunisia, (ii) the Clinical Investigation Center of the Hospitalo-Center of Sfax (CIC), Tunisia, (iii) Association de Sauvegarde des Handicapés Moteurs, Sfax (ASHMS), Tunisia, (iv) the Control and Energy Management Laboratory, University of Sfax, Tunisia, and (v) the Digital Research Center of Sfax (CRNS), Tunisia, for their supports to the success of this work.

References

[1] J. Chen, J. Wang, and W. Wang, "Robust adaptive control for nonlinear aircraft system with uncertainties," *Applied Sciences*, vol. 10, no. 12, Article ID 24270, 2020.

[2] M. Naghnaeian, P. G. Voulgaris, and N. Hovakimyan, "On robustness of L_1 adaptive control with time varying perturbations & filter design," in *Proceedings of the American Control Conference Fairmont Queen Elizabeth*, Montréal, CA, USA, June 2012.

[3] C. Rohrs, L. Valavani, M. Athans, and G. Stein, "Robustness of continuous-time adaptive control algorithms in the presence of unmodeled dynamics," *Institute of Electrical and Electronics Engineers Transactions on Automatic Control*, vol. 30, no. 9, pp. 881–889, 1985.

[4] K. Astrom, "Analysis of rohrs counterexamples to adaptive control," in *Proceedings of the The 22nd IEEE Conference Decision and Control*, pp. 982–987, San Antonio, TX, USA, December 1983.

[5] C. Cao, V. Patel, C. Reddy, N. Hovakimyan, E. Lavretsky, and K. Wise, "Are phase and time-delay margin always adversely affected by high gains?" in *Proceedings of the AIAA Guidance, Navigation, and Control Conference*, Keystone, CO, USA, August 2006.

[6] O. Naifar, G. Boukettaya, A. Oualha, and A. Ouali, "A comparative study between a high-gain interconnected observer and an adaptive observer applied to IM-based WECS," *The European Physical Journal Plus*, vol. 130, no. 5, pp. 1–13, 2015.

[7] E. Kharisov and N. Hovakimyan, "Comparison of several adaptive controllers according to their robustness metrics," in *Proceedings of the AIAA Guidance, Navigation and Control Conference*, Toronto, CA, USA, August 2010.

[8] E. Xargay, N. Hovakimyan, and C. Cao, "Benchmark problems of adaptive control revisited by L_1 adaptive control," in *Proceedings of the 17th Mediterranean Conference on Control and Automation*, pp. 31–36, Thessaloniki, Greece, June 2009.

[9] C. Cao and N. Hovakimyan, "Design and analysis of a novel L_1 adaptive controller, part i: Control signal and asymptotic stability," in *Proceedings of the American Control Conference*, pp. 3397–3402, Minneapolis, MN, USA, June 2006.

[10] C. Cao and N. Hovakimyan, "Guaranteed transient performance with L_1 adaptive controller for systems with unknown time-varying parameters and bounded disturbances: Part i," in *Proceedings of the American Control Conference*, pp. 3925–3930, New York, NY, USA, July 2007.

[11] C. Cao and N. Hovakimyan, "Design and analysis of a novel ${\cal L}_1$ adaptive control architecture with guaranteed transient performance," *Institute of Electrical and Electronics Engineers Transactions on Automatic Control*, vol. 53, no. 2, pp. 586–591, 2008.

[12] B. Maalej, A. Chemori, and N. Derbel, *$$L_1$$ adaptive control of a lower limb exoskeleton dedicated to kids' rehabilitation, New Trends in Robot Control*, pp. 107–129, Springer, Berlin, Germany, 2020.

[13] H. Rifai, M. Ben Abdessalem, A. Chemori, S. Mohammed, and Y. Amirat, "Augmented L_1 adaptive control of an actuated knee joint exoskeleton: from design to real-time experiments," in *Proceedings of the International Conference on Robotics and Automation*, Stockholm, Sweden, May 2016.

[14] M. Bennehar, A. Chemori, F. Pierrot, and V. Creuze, "Extended model-based feedforward compensation in L_1 adaptive control for mechanical manipulators: design and experiments," *Frontiers in Robotics And AI*, vol. 2, no. 32, 2015.

[15] B. Maalej, A. Chemori, and N. Derbel, "Intelligent tuning of augmented L_1 adaptive control for cerebral palsy kids rehabilitation," in *Proceedings of the International Conference on Systems, Signals and Devices*, Istanbul, Turkey, March 2019.

[16] I. Trejo-Zúñiga, S. M. Delfín-Prieto, and R. Martínez-Guerra, "Fractional controller based on a robust PIα observer for uncertain fractional systems," *International Journal of Systems Science*, vol. 50, no. 4, pp. 829–842, 2019.

[17] N. Yousfi, P. Melchior, P. Lanusse, N. Derbel, and A. Oustaloup, "Decentralized CRONE control of nonsquare multivariable systems in path-tracking design," *Nonlinear Dynamics*, vol. 76, no. 1, pp. 447–457, 2014.

[18] A. Abid, R. J. Khlif, N. Derbel, and P. Melchior, *Crone Controller Design for a Robot Arm, Book Chapter in New Developments and Advances in Robot Control*, Springer, Berlin, Germany, 2019.

[19] A. Souahi, O. Naifar, A. B. Makhlouf, and M. A. Hammami, "Discussion on Barbalat Lemma extensions for conformable fractional integrals," *International Journal of Control*, vol. 92, no. 2, pp. 234–241, 2017.

[20] R. Zhu, S. Zhang, J. Kang, Z. Guo, and G. Tang, "A modified L_1 adaptive output feedback control and its application in control of wind tunnel," in *Proceedings of the 37th Chinese Control Conference*, Wuhan, China, July 2018.

[21] G. Kaur, A. Q. Ansari, and M. S. Hashmi, "Analysis and investigation of CDBA based fractional-order filters," *Analog Integrated Circuits and Signal Processing*, vol. 105, no. 1, pp. 111–124, 2020.

[22] M. C. Tripathy, D. Mondal, K. Biswas, and S. Sen, "Experimental studies on realization of fractional inductors and fractional-order bandpass filters," *International Journal of Circuit Theory and Applications*, vol. 43, no. 9, pp. 1183–1196, 2014.

[23] T. Freeborn, B. Maundy, and A. S. Elwakil, "Approximated fractional order chebyshev lowpass filters," *Mathematical Problems in Engineering*, vol. 2015, p. 7, 2015.

[24] N. Liu, S. Cao, and J. Fei, "Fractional-order PID controller for active power filter using active disturbance rejection control," *Mathematical Problems in Engineering*, vol. 2019, p. 10, 2019.

[25] G. Boukettaya, O. Naifar, and A. Ouali, "A vector control of a cascaded doubly fed induction generator for a wind energy conversion system," in *Proceedings of the IEEE International Conference on Systems, Signals and Devices, SSD'14*, Castelldefels-Barcelona, Spain, February 2014.

[26] J. Wiora and A. Wiora, "Influence of methods approximating fractional-order differentiation on the output signal illustrated by three variants of Oustaloup filter," *Symmetry*, vol. 12, no. 11, p. 1898, 2020.

[27] S. Katoch, S. S. Chauhan, and V. Kumar, "A review on genetic algorithm: past, present, and future," *Multimedia Tools and Applications*, vol. 80, pp. 8091–8126, 2020.

[28] T. Kuang, Z. Hu, and M. Xu, "A genetic optimization algorithm based on adaptive dimensionality reduction," *Mathematical Problems in Engineering*, vol. 2020, p. 7, 2020.

[29] A. Oustaloup, F. Levron, B. Mathieu, and F. M. Nanot, "Frequency-band complex noninteger differentiator: characterization and synthesis," *Institute of Electrical and Electronics Engineers Transactions on Circuits and Systems I: Fundamental Theory and Applications*, vol. 47, no. 1, pp. 25–39, 2000.

[30] N. Hovakimyan and C. Cao, *L_1 Adaptive Control Theory: Guaranted Robustness with Fast Adaptation*, Society for Industrial and Applied Mathematics, University City, Philadelphia, 2010.

[31] M. Ghezal, M. Guiatni, I. Boussioud, and C. S. Renane, "Design and robust control of a 2 DOFs lower limb exoskeleton," in *Proceedings of the International Conference on*

Communications and Electrical Engineering, El Oued, Algeria, December 2018.

[32] L. Davis, *Handbook of Genetic Algorithms*, Van Nostrand Reinhold, New York, NY, USA, 1991.

[33] M. Mitchel, *An Introduction to Genetic Algorithms*, MIT Press, London, UK, 1998.

[34] J. A. Vasconcelos, J. A. Ramírez, R. H. C. Takahashi, and R. R. Saldanha, "Improvements in genetic algorithms," *Institute of Electrical and Electronics Engineers Transactions on Magnetics*, vol. 37, no. 5, pp. 3414–3417, 2001.

[35] Y. Miladi, M. Feki, and N. Derbel, "On the model identification of an incubator based on genetic algorithms," in *Proceedings of the International Conference On Systems, Signals And Devices*, Chemnitz, Germany, December 2012.